COMPDYN 2011
3^{rd} ECCOMAS Thematic Conference on
Computational Methods in Structural Dynamics and Earthquake Engineering
M. Papadrakakis, M. Fragiadakis, V. Plevris (eds.)
Corfu, Greece, 25-28 May 2011

SEISMIC VULNERABILITY ASSESSMENT OF MASONRY TOWERS: FULL NON-LINEAR DYNAMICS VS PUSHOVER ANALYSES

S. Casolo[1], **G. Uva**[2]

[1]Dipartimento di Ingegneria Strutturale, Politecnico di Milano
P.zza Leonardo da Vinci, 20133 Milano, Italy
e-mail: siro.casolo@polimi.it

[2] Dipartimento ICAR , Politecnico di Bari
Via E. Orabona, 4 70125 Bari, Italy
e-mail: g.uva@poliba.it

Keywords: Masonry towers, Belfry, RBSM, Pushover Analysis, Nonlinear Dynamic Analysis.

Abstract. *The paper concerns the seismic vulnerability assessment of masonry bell towers in Italy, which is performed by comparing full non-linear dynamic analysis and non-linear static analysis. An idealized case study is considered, in order to assess some basic and common features of the seismic structural response and to appraise the performance of the proposed approach. The reference model is supposed to be structurally independent, i.e. with no adjacent interacting construction. The geometrical dimensions are chosen in order to represent an average north-Italian masonry bell tower, without the intent to cover all the possible situations.*

The seismic response of these structures involves a coupling between flexural and axial vibration modes, the presence of shear damage patterns, and high vibration modes causing the belfry collapse. The problem is simplified by using a plane 2D scheme. A specific Rigid Body and Spring Model is adopted to describe the in-plane dynamics. Constitutive laws were assigned following a simplified heuristic approach including the main meso–scale damage mechanisms: i) very low tensile strength; ii) significant post-elastic orthotropy plus texture effects; iii) different rules for post-elastic axial and shear damage; iv) different dependence of the shear strength on the vertical and horizontal axial stress component; v) hysteretic energy dissipation due to cyclic loading. Even using a quite coarse mesh, the model is capable to describe the higher vibration modes with a reasonable computational effort and using realistic accelerograms. Non linear static analysis was performed, by using the RBSM model, obtaining the capacity curve and assessing the seismic demand. A comparison between the two approaches is proposed, in order to appraise the difference in the results and to evaluate quality and significance of results in terms of operational drawbacks and reduction of computational times. Particular attention is devoted to the fact that static non-linear analyses tends to neglect the damage effects induced by higher vibration modes, as well as the influence of the shear response on the global damage.

1 INTRODUCTION

In Italy, bell towers are a quite widespread architectural element, with peculiar morpho-typological characters, according to the geographic area.

A main issue in the seismic behaviour of slender masonry towers is the influence of the axial stresses induced by gravity loads, which are often close to the compression strength limit of the masonry material. Considering that historical masonry is typically characterized by complex geometry, irregularities and a high degree of inhomogeneity, stress concentrations can easily occur, which could even trigger a local collapse. Thence, the structural failure can be driven even by a moderate increase in the stress level, which can occur under seismic events or under long term loads. A notable example of the second case is represented by the sudden collapse of the Civic Tower of Pavia, Italy (about 900 years old), on 17 March, 1989 [1]. It is clear, therefore, that masonry towers are vulnerable also to low-intensity earthquakes, since static vertical loads combine with the dynamic loads induced by the ground motion.

The examination of the documentation about the damage caused by the 1976 Friuli earthquake [2] points out that in isolated bell towers damage patterns tend to be distributed all along the height, although it is frequently more severe at the base. This suggests the need of further investigations about the combined effects of flexural and axial actions, as well as the incorporation into the model of the higher vibration modes, which seem to be have a relevant role in the damage of the upper part, especially the tower crown and belfry [3].

Moreover, during strong earthquakes shear damages are also often observed, and in this case the reduction of the section stiffness (i.e. the loss of validity of the Eulero–Bernoulli hypothesis of plane cross-section) can significantly affect the overall response of the structure. Specific approaches are needed in order to deal with these aspects, and in particular it is paramount to model the non-symmetry in tension and compression that characterise the masonry material of which these structures are composed [4].

Finally, the investigation of the response to very strong earthquakes requires to describe the effects of the damages that cause a remarkable reduction of the material stiffness, as well as the dissipation of the seismic energy through repeated cycles of plastic deformation [5, 6]. When the tower is not particularly slender, and depending on the frequency content of the forcing actions, a material model which is capable to describe both the axial and the shear response and damage under cyclic loading is also required in order to investigate the global shear damage effects [7, 8, 9].

2 THE RBSM MODEL

The non linear behaviour of the slender medieval towers is studied by means of a specific mechanistic model made by rigid bodies and springs, RBSM which considers only the in-plane dynamics. This model is capable of describing the higher mode of vibration, as well as the combined axial and shear deformation and damage of the material by means of a simplified heuristic approach. The rigid element method (REM) [10] idealises the masonry structure as a mechanism made of rigid elements and springs. The elements are quadrilateral and have the kinematics of rigid bodies with two linear displacements and one rotation, as shown in Figure 1(b). Three springs devices connect the common side between two rigid elements or the restrained sides, as shown in Figure 1(c). These connections are two axial springs k^P and k^R, placed in the point P and R separated by a distance $2b$, and one shear device k^Q placed in the middle of the side. A volume of pertinence V^P, V^Q and V^R is assigned to each connection point. The elastic characteristics of the connecting devices are assigned with the criterion of

approximating the strain energy of the corresponding volumes of pertinence in the cases of simple deformation.

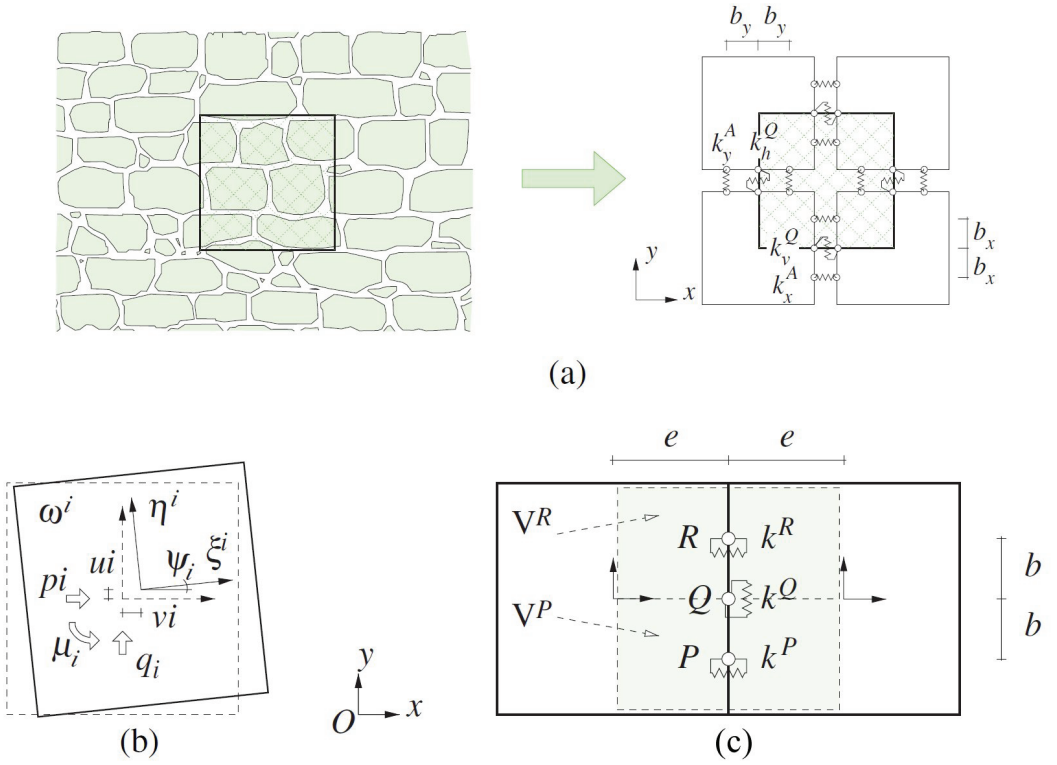

Figure 1: Scheme of a unit cell defined by four rigid elements(a), kinematics (b), disposition of the connecting spring-devices between a couple of rigid elements (c) for macroscale modelling of a representative volume of masonry [10, 11].

The conceptual core of this model is the macroscopic unit cell defined by four quadrilateral rigid elements connected to each other as shown in Figure 1(a). The cell size should be equal or larger than the minimum representative volume (RVE) of the heterogeneous solid material. In particular, the orthotropy of the shear response and the local mean rotation of the blocks, which depend on the different geometric arrangement of the vertical and horizontal material joints as well as the shape and size of the original blocks, are features that can be accounted at the macro-scale [11].

Out-of the linear elastic field, the main macroscopic constitutive aspects are: the very low tensile strength; the significant post-elastic orthotropy combined with the texture effects; the dependence of the shear strength on vertical compression stress; the progressive mechanical degradation during repeated loading; and the energy dissipation capability. To do this, a simplified heuristic approach is proposed, based on the phenomenological consideration of the main in-plane damage mechanisms that can be described at the meso–scale by adopting specific separate hysteretic laws for the axial and shear deformation between the elements. This separation reduces the computational effort, even though a Coulomb-like law is adopted in order to relate the strength of the shear springs to the vertical axial loading.

In the present work, different behaviours have been attributed to the shear connections along the vertical and horizontal directions, somewhat in the spirit of a Cosserat non-linear solid continuum material [11]. Two axial, one shear, and two in-plane flexural loadings are considered for

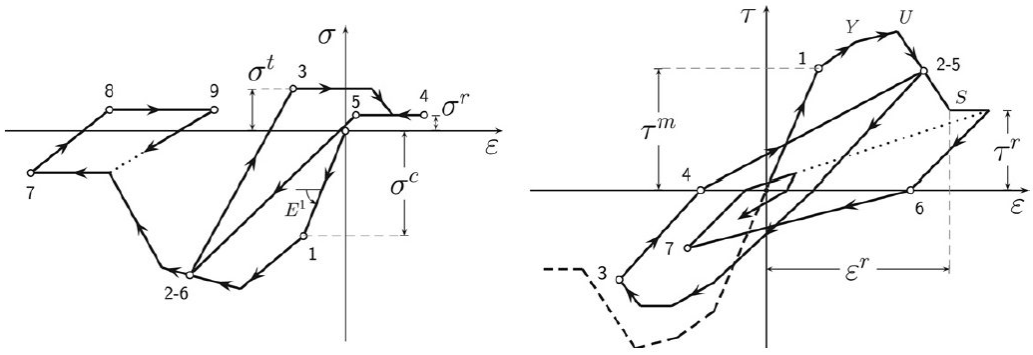

Figure 2: Schematic representation of the hysteretic rules for the axial (on the left), and the shear connecting springs (on the right).

the parameter identification [10]. The monotonic and hysteretic constitutive laws are assigned to the connecting devices adopting a phenomenological approach and separate phenomenological descriptions of the hysteresis behaviour of the axial and shear connections, as schematically shown in Figure 2. These laws are based on experimental monotonic and cyclic tests available in literature, and should be assigned to rigid elements whose size is approximately comparable to the test specimens in order to limit the problems with size effect. The plastic response of each axial connection is independent from the behaviour of any other connection, while the shear strength is related to the stresses of the axial connections according with Coulomb criterion.

It is worth noting the true discrete character of this model. In fact, during loading, relative motion between two adjacent elements always occurs, with overlapping, separation or sliding between two adjacent rigid elements; numerically, this means compression, tension or shear in the volume of pertinence of the connecting devices. This notwithstanding, the initial contacts do not change during the analysis and the global mechanism maintains the initial connectivity in order to reduce the computational effort.

3 THE REFERENCE TOWER

An idealized case study has been considered, in order to assess some basic and common features of the structural response to seismic actions and to appraise the performance of the approach proposed for the modelling. Such a reference model has been supposed to be structurally independent, i.e. with no adjacent interacting construction, and characterized by geometrical regularity both in plan and in elevation. The dimensions were chosen by looking at a number of significant examples (Fig. 3), in order to represent an average masonry bell tower located in seismic zones of Northern Italy, without the intent, of course, to cover all the possible situations. Of course, the geometry of the model was simplified by disregarding the typical structural details, like – for example – the presence of internal vaults.

On the basis of these observations, it was designed an ideal tower having a 5.30 x 5.30 m square base, with a wall thickness varying from 1.00 m at the base to 0.85 m at the top, and having a total height of 28.50 m. In Figures 4 and 5, the 3D drawings and the schematic sections and plans of the tower are shown, and the geometrical characteristics are summarized in Table 1.

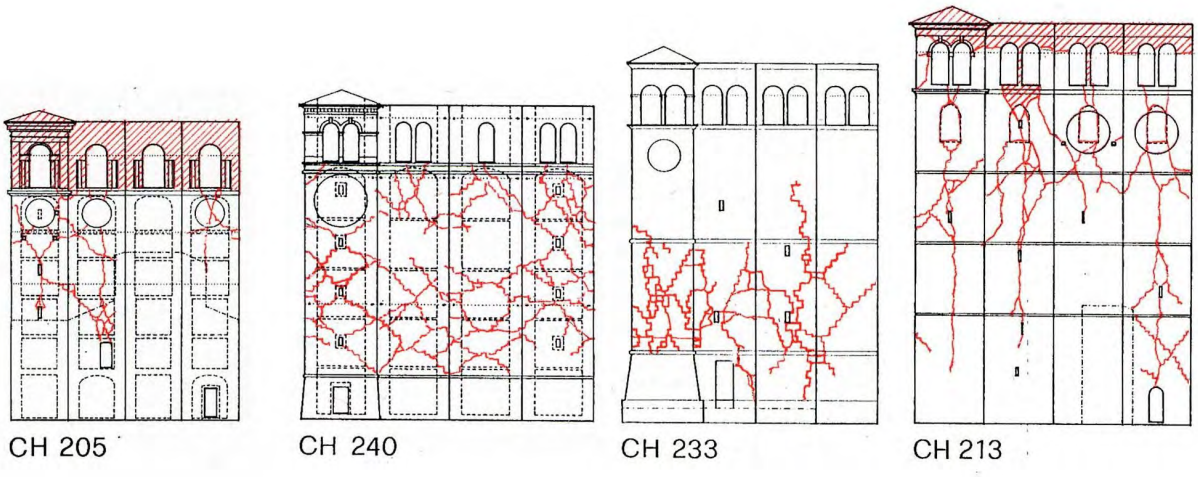

Figure 3: Some typical geometry and damage patterns of Italian bell-towers [2].

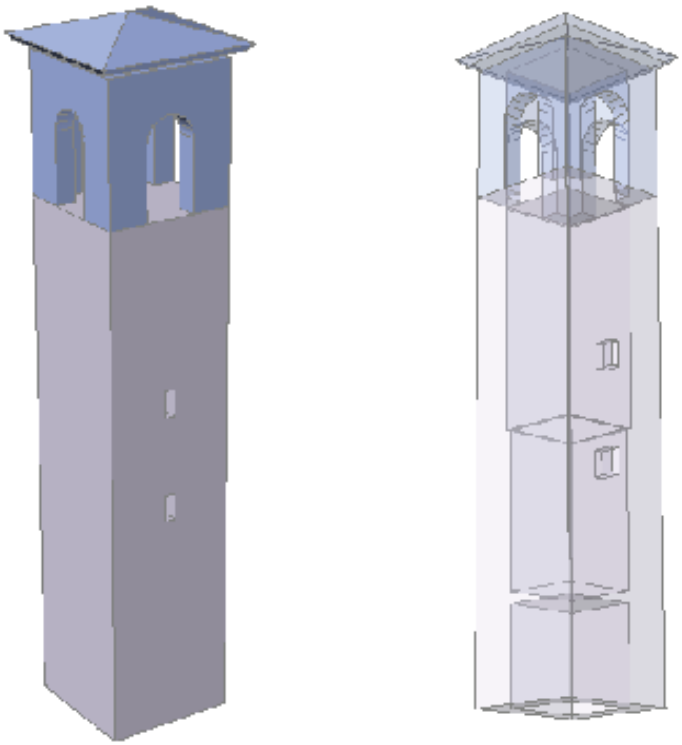

Figure 4: 3D drawing of the reference tower.

Table 1: Geometrical characteristics of the reference tower.

Total height (H)	$28.50\ m$
Base (LxL)	$5.30\ m$ x $5.30\ m$
Base wall Thickness (t)	$1.00\ m$
Wall mass density (ρ)	$1900\ kg/m^3$
Damping (ξ)	0.05

3.1 Mechanical parameters of the masonry material

According to the constitutive model adopted for the axial and shear springs (Par. 2), a set of parameters are needed in order to define the corresponding skeleton curves and hysteretic rules [7]. The values assigned to the relevant parameters to define the masonry material of the reference tower are: compressive stress at the elastic limit: $1\ MPa$; peak compressive strength: $2\ MPa$; residual compressive strength: $0.2\ MPa$; peak tensile strength: $0.2\ MPa$; residual tensile strength: $0.02\ MPa$; shear value at the elastic limit: $0.088\ MPa$; peak shear strength on the horizontal plane: $0.097\ MPa$; peak shear strength on the vertical plane: $0.165\ MPa$; residual shear strength: $0.02\ MPa$ friction coefficient on the horizontal plane: 0.25; friction coefficient on the vertical plane: 0.05.

3.2 Preliminary characterization of the tower

Preliminarily, the analysis of the bell–tower under the only gravity loads was performed (the non structural permanent loads and the service loads were not considered, since they represent a negligible quote of the total loads). The maximum vertical displacement in this loading condition is $2\ mm$. In Figures 12, 13, 14, 15, at the left, are respectively shown the deformed shape, the normal stress map (S_{22}), the shear strain along horizotnal direction (E_{12}), the shear strain along vertical direction (E_{21}).

Then the first 3 vibration modes of the tower were determined. The corresponding natural periods are reported in Table 2 and the modes shape are shown in Figure 6.

Table 2: Natural periods of vibration of the first three modes.

Mode ♯	Period	Type
1	$0.517\ s$	1^{st} flexural
2	$0.128\ s$	2^{nd} flexural
3	$0.079\ s$	1^{st} axial

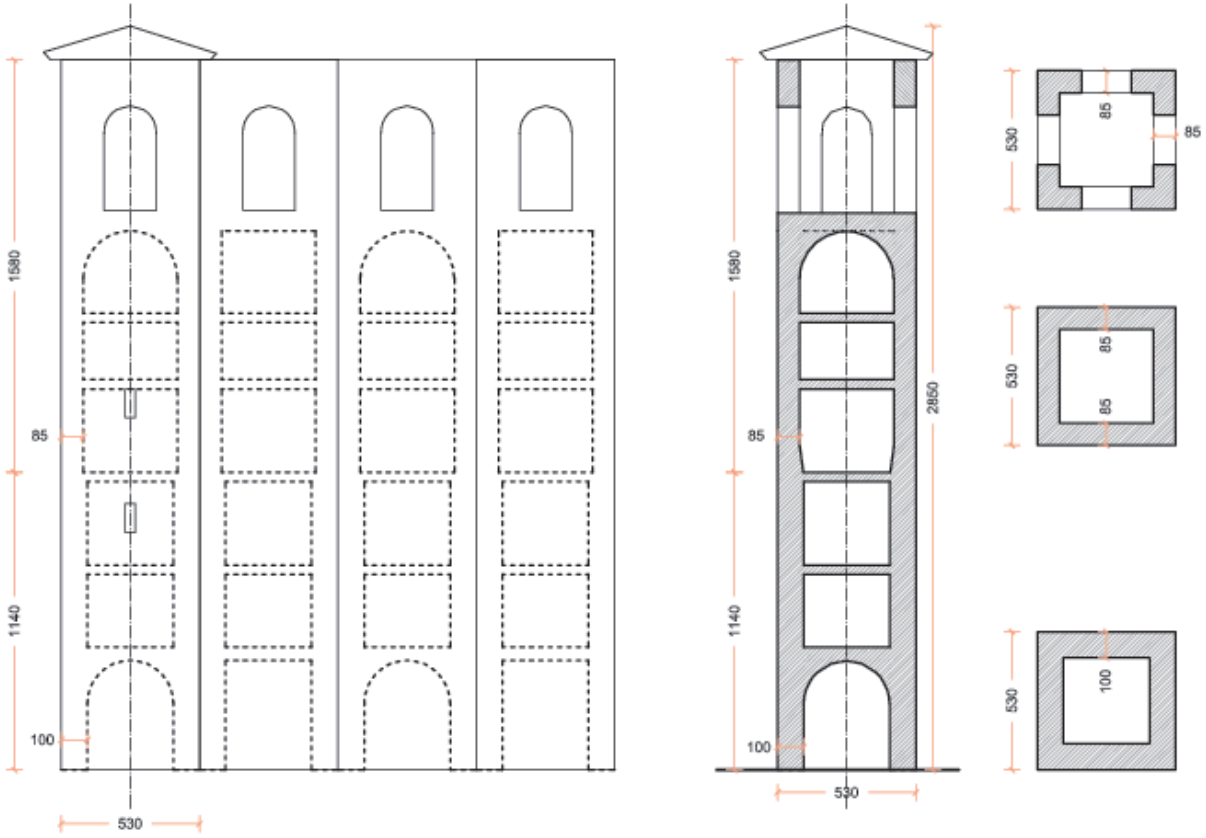

Figure 5: Schematic prospects, section and plan views of the idealized case study.

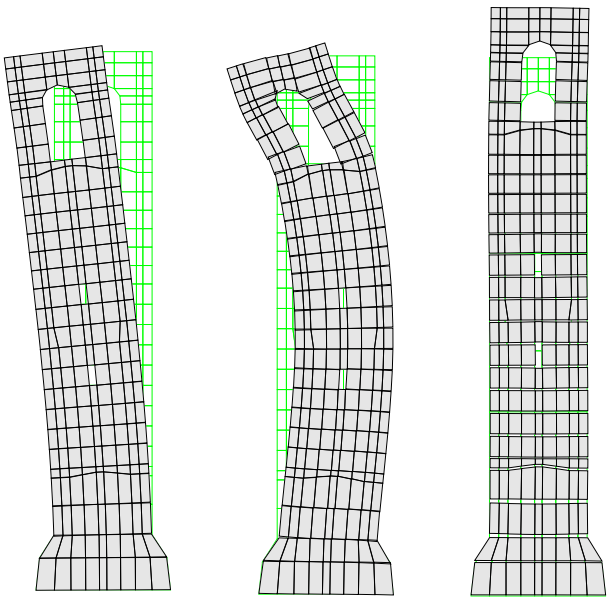

Figure 6: The first three mode shapes.

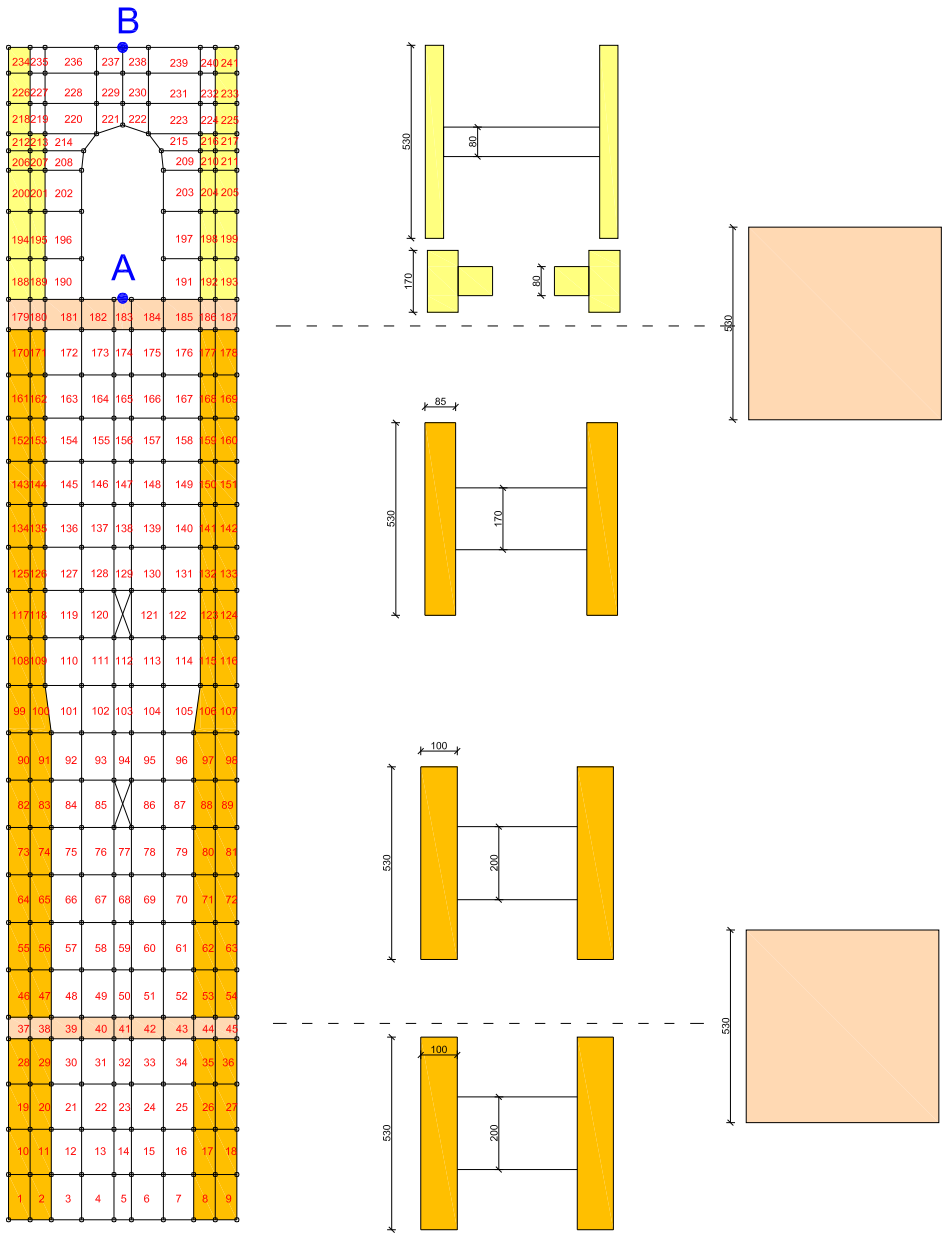

Figure 7: The mesh of the reference tower used in the numerical simulations by RBSM. The control point B, located at the top of the belfry is also shown.

4 NON LINEAR METHODS: NON LINEAR DYNAMIC VS NONLINEAR STATIC ANALYSIS

Step-by-step nonlinear dynamic analysis is hardly used in the practical application, although it is definitely the most complete and realistic approach for seismic analysis. Indeed, it presents a number of drawbacks, which actually restrict its use to advanced users and very specific case studies: adequate numerical codes, even commercial ones, are not easy available, or introduce too many complications for average end-user; the definition of the model, especially with regard to the constitutive aspects (the post-elastic, hysteretic behaviour of the structure, and the consequent energy dissipation, should be consistently reproduced) is critical; the choice of significant input accelerograms is still a controversial question; the computational cost is very high; the uncertainty about input data strongly influence the reliability of the results. Anyway, in order to predict the nonlinear structural response under strong ground motions, in the last few years simplified procedures have been proposed aimed at performing non linear analysis in a static context (Nonlinear Static Procedures - NSP), where the problem can be more easily managed, and numerical tools with a high circulation are available. These methods, generally known as pushover analyses, have recently assumed a large relevance, especially for the assessment of existing buildings [12]. In these procedures, basically, a computational model of the structure is loaded up with a proper distribution of horizontal static loads, which are gradually increased with the aim of "pushing" the structure into the nonlinear field. The basic idea is that the resulting response conveniently represents the envelope of all the possible structural responses, and can so be used to replace a full nonlinear dynamic analysis. When speaking of historical and monumental buildings, the question is even more critical: nearly all the structural analysis methods suffer from a lot of uncertainties and limitations, mainly derived from the incompleteness of the knowledge level, from the presence of widespread inhomogeneities and nonlinearities, and a complex constructive history.

4.1 Nonlinear Dynamic analyses with design–consistent artificial accelerograms

The full dynamic analyses were performed by using artificial accelerograms to represent the ground motions.

The reference design spectra used are those for the Ultimate Limit State of Life Safety for the zones 1, 2, 3 and 4 in which the Italian territory is classified, assuming an "A"–type soil and no topographic amplification effect (this corresponds to a probability of exceedance $P_{VR} = 10$ in 50 years, i.e. to a return period of the seismic action $T_R = 475$ years).

For each zone, the artificial accelerograms were generated according to the procedure proposed by Sabetta and Pugliese [13]. The resulting accelerograms have been further processed in order to improve the matching with the spectrum.

It will be now presented, as an example, the results of the analyses performed by using 4 accelerograms, one for each of the average hazard level in Italy. In Figures 11, 10, 9, 8 the input accelerograms used respectively for Zone 1, 2, 3 and 4 are shown. In the same figures, some significant outputs of the analyses are also shown: the displacement time-history for two representative points: the control point B, located at the top of the belfry and point A, at the base of the belfry (see Fig. 7); the plot of the base shear against the mean displacement of points A and B; the time hystory of the dissipated energy. For each zone, the deformed shape at the end of the dynamic analysis have been plotted in Figure 12, and also the vertical normal stress (Fig. 13), the horizontal shear stress (Fig. 14) and the vertical shear stress (Fig. 15).

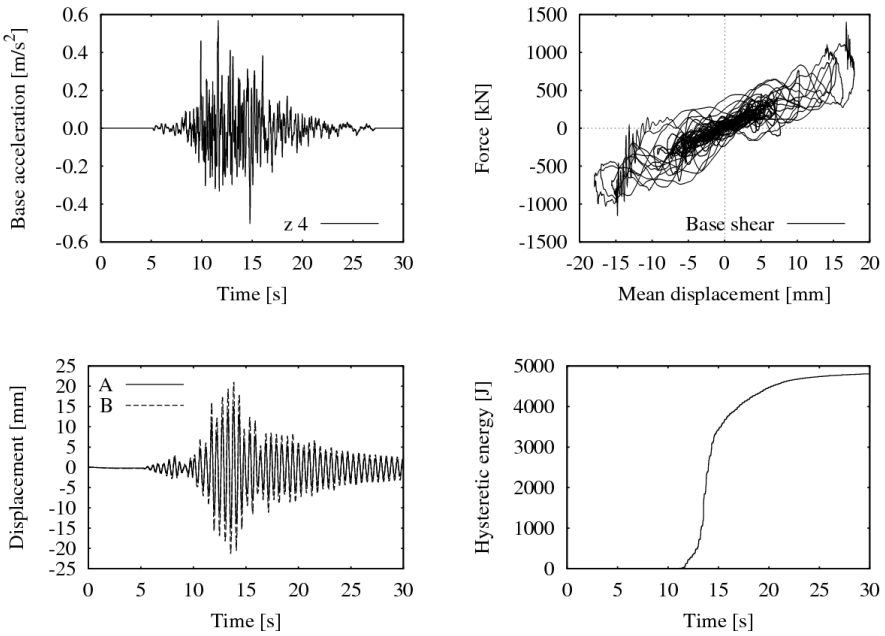

Figure 8: Input artificial accelerogram used for Zone 4; displacement time-history for points A and B (see Fig. 7); Base shear–mean displacement (points A, B) relationship; Hysteretic energy time history.

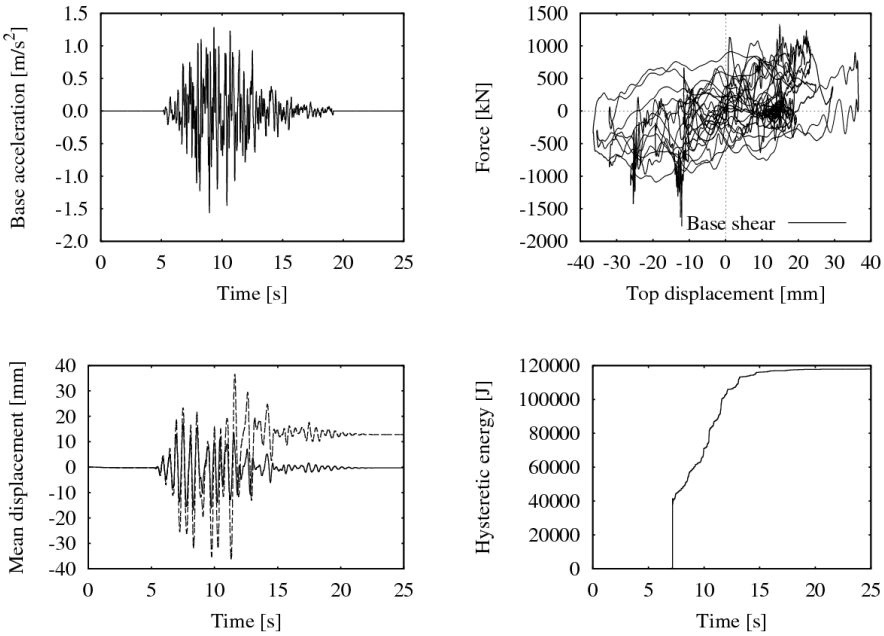

Figure 9: Input artificial accelerogram used for Zone 3; displacement time-history for points A and B (see Fig. 7); Base shear–mean displacement (points A, B) relationship; Hysteretic energy time history.

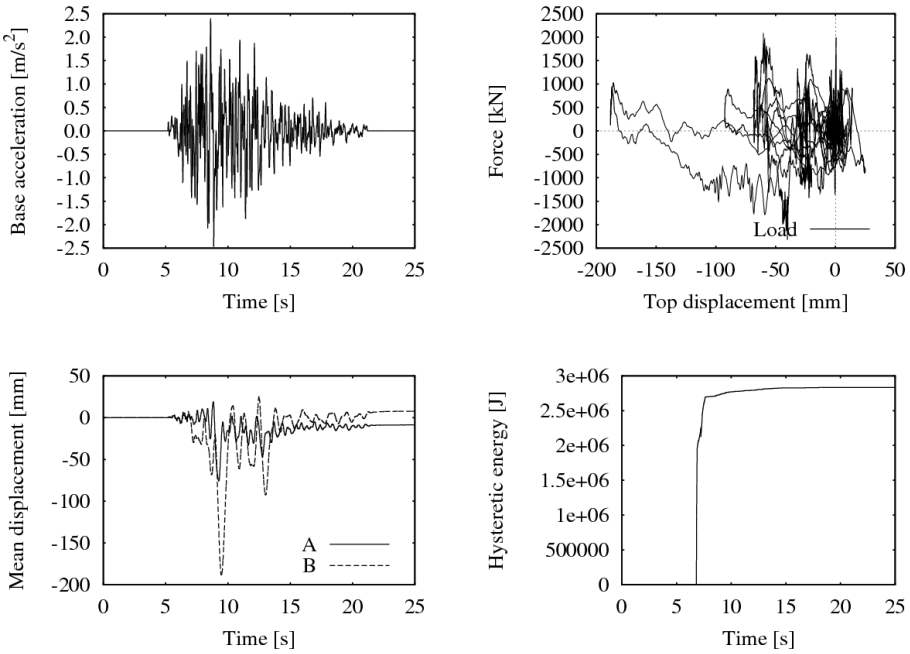

Figure 10: Input artificial accelerogram used for Zone 2; displacement time-history for points A and B (see Fig. 7); Base shear–mean displacement (points A, B) relationship; Hysteretic energy time history.

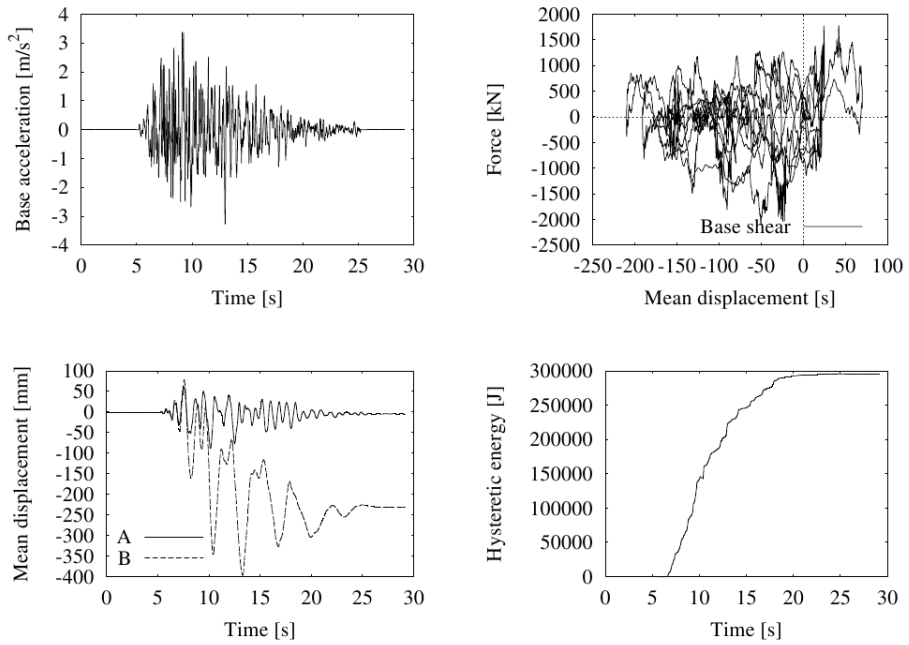

Figure 11: Input artificial accelerogram used for Zone 1; displacement time-history for points A and B (see Fig. 7); Base shear–mean displacement (points A, B) relationship; Hysteretic energy time history.

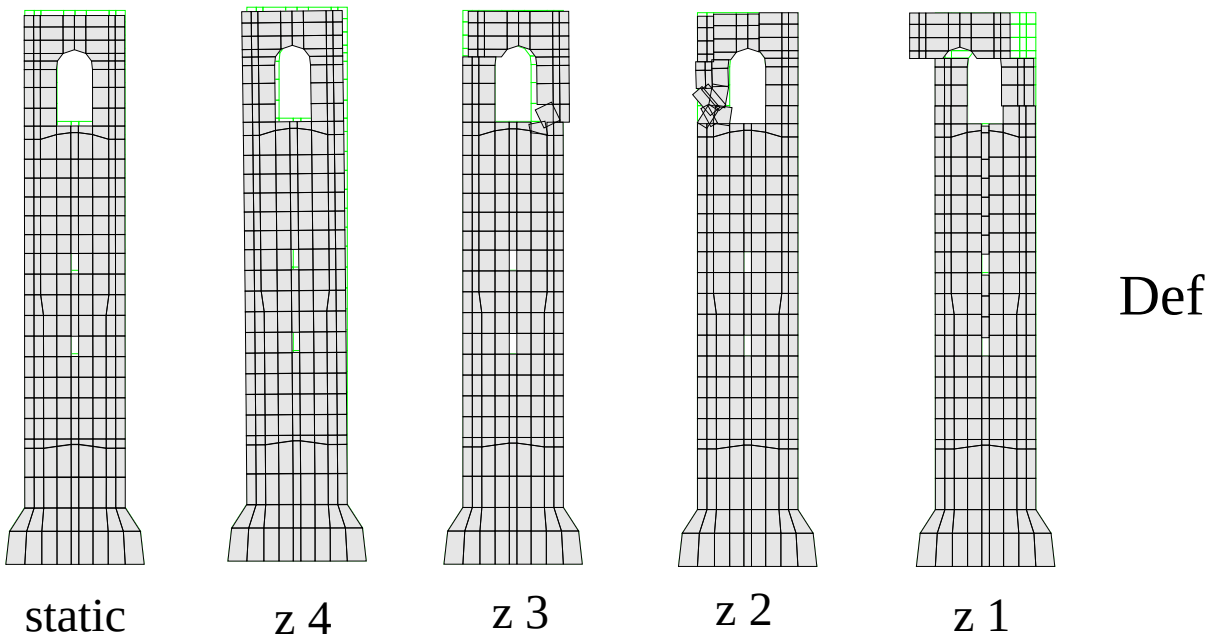

Figure 12: Deformed shapes for the static loading condition and at the end of full-dynamic analyses (Zone 4, 3, 2, 1).

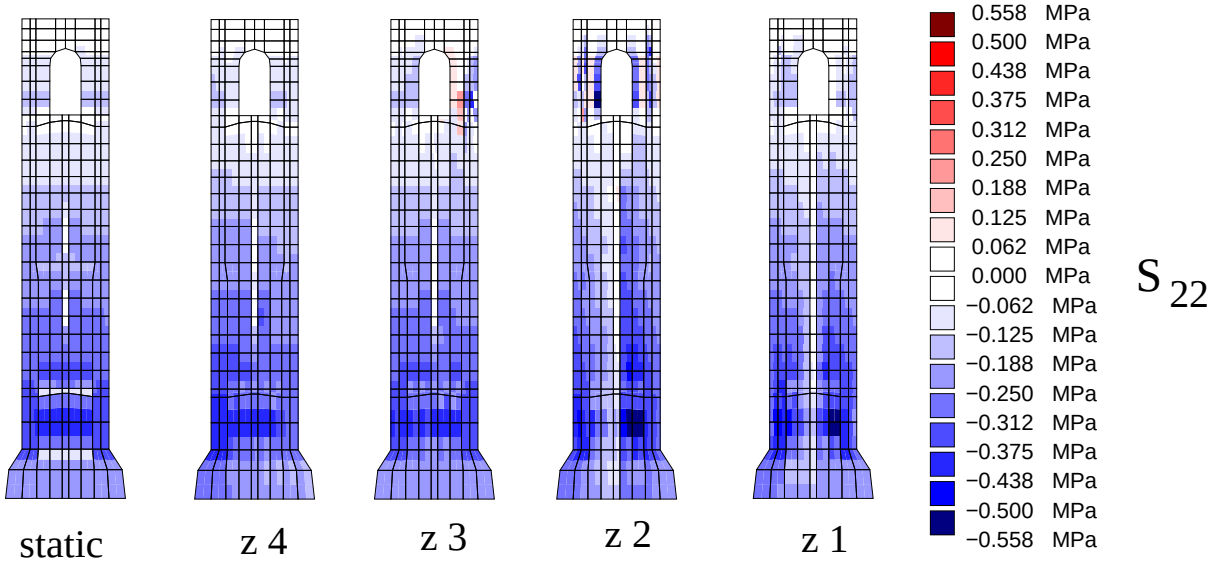

Figure 13: Normal stress along vertical direction (S_{22}) map: static load condition; ND analyses in Zones 4, 3, 2, 1.

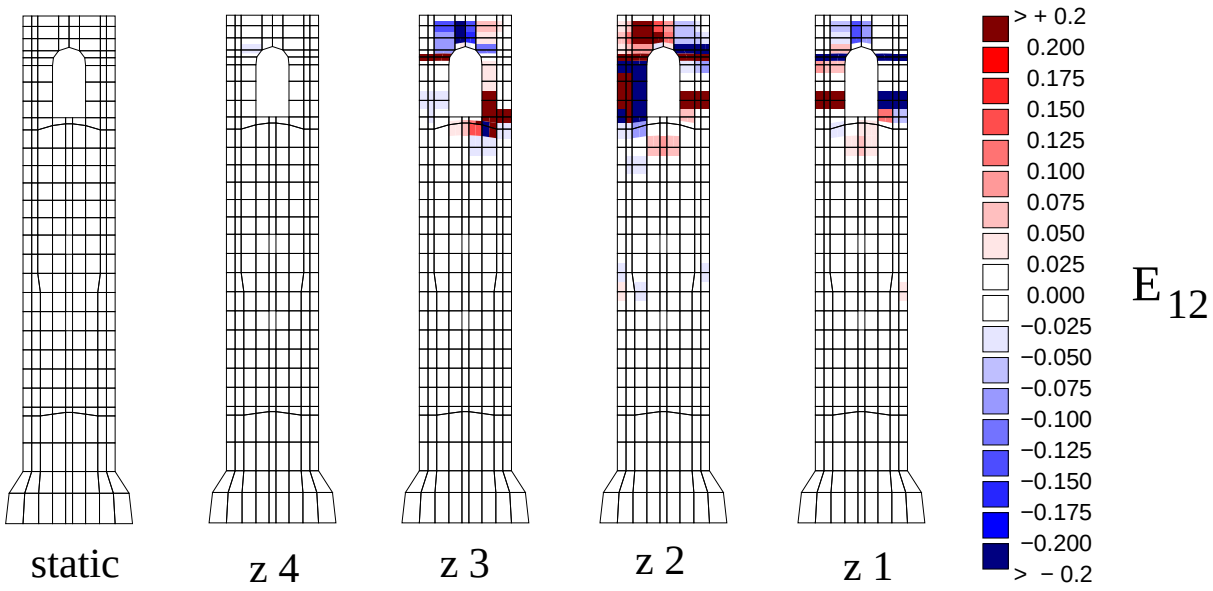

Figure 14: Shear strain along horizontal direction (E_{12}): static load condition; ND analyses in in Zones 4, 3, 2, 1.

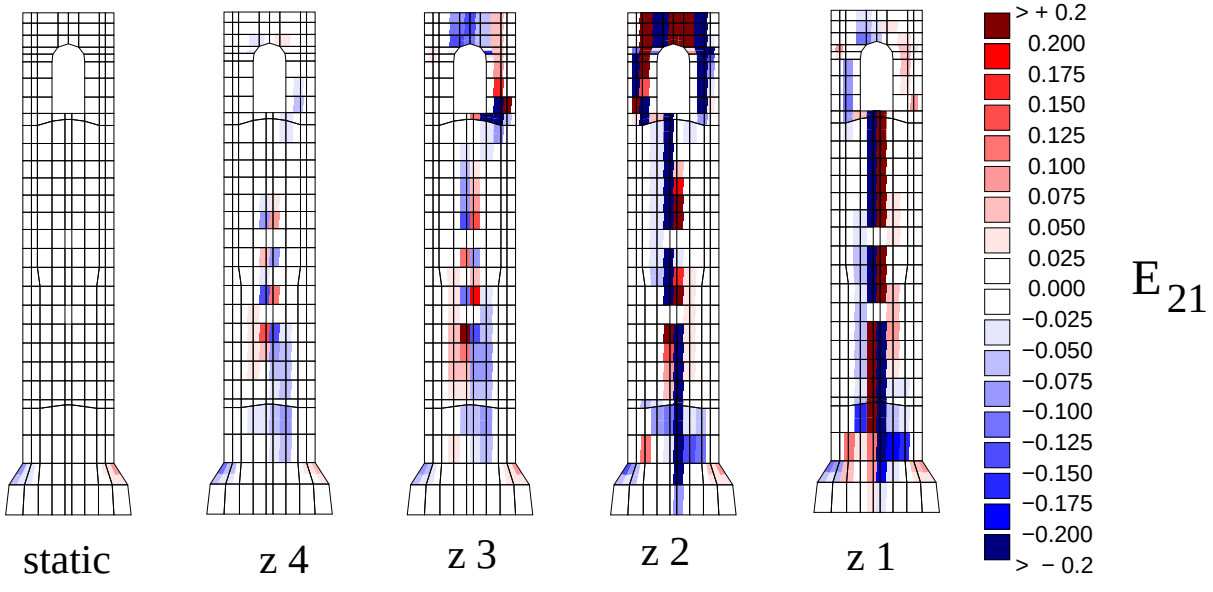

Figure 15: Shear strain along vertical direction (E_{21}): static load condition; ND analyses in Zones 4, 3, 2, 1.

The results reported in the figures clearly show the development of a global shear mechanism of damage for the tower. In Zone 4 (low seismic hazard) such a mechanism can already be appraised: by looking at Figure 15, it can be seen that the in the lower part of the tower are present significant vertical shear strains in the middle section. The relevance of the global shear collapse mechanism is progressively more evident when considering the accelerogram related to the zones 2 an 1. This is also confirmed by the normal stress map, which shows that the tower is almost split into two separate portions. This is also visible in the deformed shape of Figure 12, where, in the central thin strip, consistent vertical displacements can be observed, which suggest that a failure of the central strip has occurred .

As a consequence of this failure mode, a permanent tilt occurs for all the accelerograms. This can be clearly seen from the displacement time history of point B (Figures 8, 9, 10, 11).

For Zone 4, the permanent tilt is clearly visible in Figure 12, whereas in the other cases it is not evident because of the different metric scale adopted. In fact, for the accelerograms of zones 3, 2 and 1 there is an additional partial collapse mechanism that is activated: the failure of the belfry. The figure 14 shows the development of shear strains on the horizontal plane at the base and top of the belfry, whereas the deformed shape indicates the permanent slidings and rotations suffered by the element: actually it can be said that in these conditions the belfry is collapsed.

4.2 The pushover simulation

The non linear static analysis of the tower is now proposed, following the methods included in the European codes [12], which are based on the well-known "N2 method" [14]. The aim is to perform a critical comparison with the full dynamic analysis, appraising the reliability and relevance of the results. Analyses were performed by applying two different vertical distributions of the lateral loads: a "uniform" pattern (which will be hereafter referred to as "mode 0"), based on lateral forces that are proportional to mass regardless of elevation (uniform response acceleration); a "modal" pattern (which will be hereafter referred to as "mode 1") corresponding to a distribution of the acceleration proportional to the 1st modal shape.

During the loading process the displacement d_c of the control point B (Fig. 7) was monitored in order to trace the pushover curve in terms of the equivalent lateral force F_b, obtaining the generalized force-displacement relationship: $F_b - d_c$.

The ultimate limit state verification then consists in checking out that the ultimate displacement capacity is larger than the corresponding displacement required by the design seismic action. It is hardly worth observing that in order to perform a nonlinear analysis, even if a static one, a proper numerical code is needed (for instance, a FE code) as well as nonlinear constitutive laws for the materials and the structural elements, able to reproduce the strength and stiffness degradation suffered by the damaged elements. Indeed, the idea of handling a nonlinear static analysis in order to take into account –at least in a simplified way– the inelastic characteristic of the structure was suggested by the availability of codes able to provide these kind of models, whereas the requirements for dynamic analyses are rather oriented to specialist users. It should be anyhow remarked that some operational drawbacks still exist, and even in the most advanced numerical formulations, it is frequent to encounter troubles in the reconstruction of the equilibrium path. In the case study, the pushover analyses were carried out by using the RSBM described in Par. 2.

The methodology includes the following steps: i) transformation of the pushover curve into a simplified bilinear force-displacement relationship for an equivalent SDOF system; ii) definition of the inelastic seismic demand for such SDOF system in the acceleration–displacement

(AD) format; iii) transformation of the displacement demand (i.e. the "target" displacement) for the SDOF system into the corresponding maximum displacement of the original structure; iv) verification of displacement compatibility (according to the current standards, for masonry structures only the global displacement checking is required, and not a specific assessment of single structural elements).

In Figure 16 the results obtained at the end of the pushover analysis performed under the modal pattern are reported: deformed shape; normal stress map; shear deformations along Y–axis; shear deformations along X–axis. The deformed shape at the end of the analysis and the

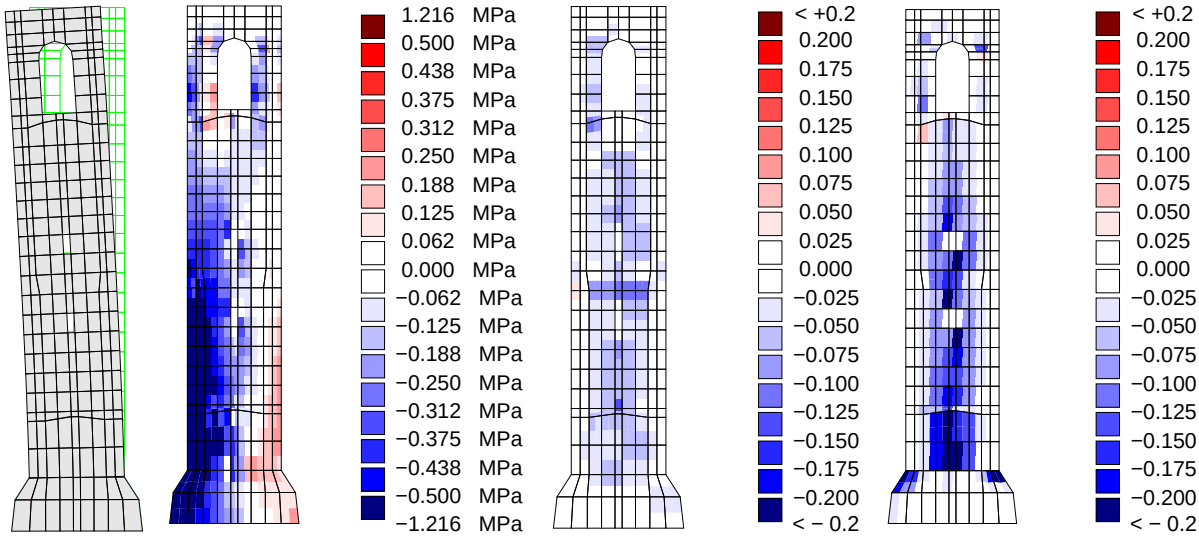

Figure 16: From left to right: results of the pushover analysis: final deformed shape; vertical axial stress; shear strain along vertical direction; shear strain along horizontal direction.

corresponding maps of the axial stresses and shear deformations reveal that the collapse point is characterized by a global shear mechanism, whereas local damages involving the belfry are negligible.

In Figure 17, the curve expressing the base reactions F_b vs the characteristic displacement d_c of the tower is shown for the loading pattern 1 (distribution of accelerations proportional to the first modal shape), which resulted to be the most demanding condition, together with the force-displacement relationship for the SDOF equivalent system ($F^* - -d^*$) , obtained by applying the modal participation factor Γ:

$$F^* = \frac{F_b}{\Gamma}; \qquad d^* = \frac{d_c}{\Gamma} \qquad \Gamma = \frac{\Sigma m_i \Phi_i}{\Sigma m_i \Phi_i^2} = 1.79 \tag{1}$$

(Φ is the 1^{st} modal shape of the structure).

The characteristic curve F^*–d^* was then transformed into the bilinear simplified relationship, also plotted in Figure 17, characterized by the yield force $F_y^* = 583.8\ KN$, by the ultimate displacement $d_u^* = 19.92\ mm$ and by the displacement at yielding $d_y^* = 15.90\ mm$ (transformation is based on an equal–energy criterion).

The elastic design spectrum in AD format is a parametric function of the natural period T^*: ($S_{de}(T^*)$, $S_{ae}(T^*)$). Thence, for the idealized bilinear system ($T^* = 0.522$ s, $m^* = \Sigma m_i \Phi_i$), the acceleration demand (strength) in the case of a perfectly elastic behaviour, and the corresponding elastic displacement demand, can be singled out. The inelastic seismic demand is

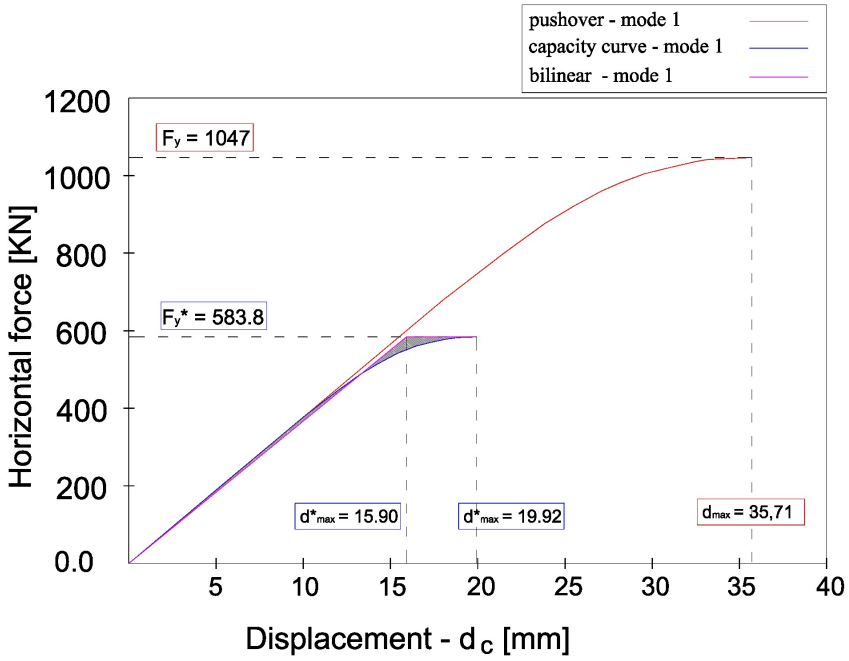

Figure 17: The pushover curve of the tower (mode 1 load pattern), the capacity curve and the equivalent bilinear curve of the equivalent SDOF system.

henceforth defined by accounting for the system ductility, depending on the range of the spectrum in which the system's period falls. The watershed is represented by the characteristic period of the ground motion T_C, defined as the transition period from the constant acceleration branch of the spectrum to the constant velocity one.

If $T^* \leq T_C$, the displacement response of the inelastic system is larger than the equal period elastic one, and can be evaluated by the following expression:

$$d^*_{\max} = \frac{d^*_{\mathrm{e}\max}}{q^*}\left(1 + (q^* - 1)\, T^*/T_C\right) \geq d^*_{\mathrm{e}\max} \qquad \text{where} : q^* = S_{ae}(T^*)\; m^*/F^*_y \tag{2}$$

The factor q^* represents the ratio between the force corresponding to a linear elastic response and the yielding force of the equivalent system (it will be always assumed $q^* \geq 1$).

If, instead, $T^* \geq T_C$, like in this case, the equal displacement rule applies: the inelastic displacement demand $S_d(T^*)$ is assumed to be the same as the elastic system having the same period: $d^*_{\max} = d^*_{\mathrm{e}\max} = S_{de}(T^*)$, where $S_{de}(T^*) = S_{ae}(T^*)\,(\frac{T^*}{2\,\pi})^2$.

Eventually, the displacement demand for the original structure is $d_{\max} = \Gamma d^*_{\max}$, and can be compared with the available ductility provided by the pushover analysis (Fig. 17): $d_u = 35.71\ mm$.

In Table 3 the results obtained for the four seismic design zones are reported in terms of the elastic spectral acceleration, the factor $q*$, the maximum inelastic displacement $d^*_{\max}$ of the equivalent system, and the maximum displacement d_u of the tower.

Table 3: Target displacements and actual available displacements of the structure for the different zones for the modal load distribution.

	Zone 4	*Zone 3*	*Zone 2*	*Zone 1*
$S_{ae}(T^*)$	$6.58\ m/s^2$	$4.70\ m/s^2$	$2.82\ m/s^2$	$0.94\ m/s^2$
$d^*_{et} = d^*_t$	$4.55\ cm$	$3.25\ cm$	$1.95\ cm$	$0.65\ cm$
d_u		$3.57\ cm$		

5 FINAL REMARKS

The use of the RSBM approach [10] is particularly effective for performing in-plane dynamic analyses. In the present work, its application for the seismic assessment of bell-towers has allowed to investigate the structural response under accelerograms corresponding to different levels of hazard, and to perform a nonlinear static analysis, in order to compare two different approaches.

In particular, an interesting result was related to the possible development of different collapse mechanisms. Actually, the main evidence is that while the dynamic analyses provide the presence of a local failure mode involving the belfry, which is a particularly vulnerable element of bell–towers, the pushover analyses only encounter a global shear failure mode. So, even if the results of the assessment performed in displacements terms (seismic demand vs available displacement) supplied by the nonlinear static procedure are quite comparable with the dynamic ones, the information about the damage modes is much poorer. The pushover procedure, indeed, doesn't seem to be able to describe the effect induced by earthquakes on the belfry, which are related to the higher vibration modes.

REFERENCES

[1] L. Binda, G. Gatti, G. Mangano, C. Poggi, G. Sacchi Landriani, The collapse of the civic tower of pavia: a survey of the materials and structure, Masonry International 6 (1) (1992) 11–20.

[2] F. Doglioni, A. Moretti, V. Petrini, Le Chiese e il Terremoto, Lint press, Trieste, 1994, in Italian.

[3] E. Curti, S. Lagomarsino, S. Podest, Dynamic models for the seismic analysis of ancient bell towers, in: P. Loureno, P. Roca, C. Modena, S. Agrawal (Eds.), Structural Analysis of Historical Constructions SAHC-2006, MacMillan, New Delhi, India, 2006.

[4] G. Uva, G. Salerno, Towards a multiscale analysis of periodic masonry brickwork: A fem algorithm with damage and friction, International Journal of Solids and Structures 43 (13) (2006) 3739 – 3769. doi:10.1016/j.ijsolstr.2005.10.004.

[5] S. Casolo, A three-dimensional model for vulnerability analysis of slender medieval masonry towers, Journal of Earthquake Engineering 2 (4) (1998) 487–512.
URL http://www.informaworld.com/10.1080/13632469809350332

[6] G. Magenes, G. Calvi, Cyclic behaviour of brick masonry walls, in: Proceedings of the 10^{th} World Conference on Earthquake Engineering, Madrid, 1992, pp. 3517–3522.

[7] S. Casolo, F. Peña, Rigid element model for in-plane dynamics of masonry walls considering hysteretic behaviour and damage, Earthquake Engineering & Structural Dynamics 36 (8) (2007) 1029–1048. doi:10.1002/eqe.670.

[8] S. Casolo, F. Peña, Dynamics of slender masonry towers considering hysteretic behaviour and damage, in: M. Papadrakakis, D. Charmpis, N. Lagaros, Y. Tsompanakis (Eds.), ECCOMAS-COMPDYN, Thematic Conference on Computational Methods in Structural Dynamics and Earthquake Engineering, Crete, Greece, 2007.

[9] F. Peña, P. B. Lourenço, N. Mendes, D. V. Oliveira, Numerical models for the seismic assessment of an old masonry tower, Engineering Structures 32 (5) (2010) 1466 – 1478. doi:10.1016/j.engstruct.2010.01.027.

[10] S. Casolo, Modelling in-plane micro-structure of masonry walls by rigid elements, International Journal of Solids and Structures 41 (13) (2004) 3625–3641. doi:10.1016/j.ijsolstr.2004.02.002.

[11] S. Casolo, Macroscopic modelling of structured materials: Relationship between orthotropic cosserat continuum and rigid elements, International Journal of Solids and Structures 43 (3-4) (2006) 475 – 496. doi:10.1016/j.ijsolstr.2005.03.037.

[12] Eurocode 8: Design of structures for earthquake resistance- part 1: General rules, seismic actions and rules for buildings.

[13] F. Sabetta, A. Pugliese, Estimation of response spectra and simulation of non-stationary earthquake ground motion, Bull. Seism. Soc. Am. 36 (2) (1996) 337–352.

[14] P. Fajfar, A nonlinear analysis method for performance-based seismic design, Earthquake Spectra 16 (3) (2000) 573–592. doi:10.1193/1.1586128.